PROCEEDINGS OF THE YEREVAN STATE UNIVERSITY

Chemistry and Biology 2025, **59**(3), p. 95–104

Chemistry

EXTRACTION OF TRIMETHYLBENZOYL DIPHENYLPHOSPHINE OXIDE FROM THE CURED PEGDA-HYDROXYAPATITE BONE GRAFT

M. S. TOROSYAN [1,2*]

[1] *Chair of Pharmaceutical Chemistry and Pharmacognosy, Institute of Pharmacy, YSU, Armenia*
[2] *A.B. Nalbandyan Institute of Chemical Physics, NAS of the RA, Armenia*

Currently, personalized implants are becoming increasingly interesting topic, with additive manufacturing being one of the most effective solutions. Numerous research papers focus on enhancing mechanical properties while maintaining biocompatibility. A frequently utilized polymer in implant printing is polyethylene glycol diacrylate (PEGDA), which is additionally employed as a scaffold for antibiotics to prevent oral consumption and reduce the negative side effects of antibiotics on the human body. One of the most common photoinitiators used to polymerize the PEGDA is trimethylbenzoyl diphenylphosphine oxide (TPO), which is hazardous. This study aims to explore a technique for the selective removal of TPO from an implant to reduce the potential hazard, ensuring that the antibiotic remains intact. Two solvents were utilized: saline and a 96% ethanol solution. Consequently, ethanol demonstrated improved extraction efficiency of TPO from the polymer matrix, while maintaining the antibiotic content. This demonstrates that the TPO can be selectively extracted from the implant, thereby minimizing potential risks.

https://doi.org/10.46991/PYSUB.2025.59.3.095

***Keywords*:** trimethylbenzoyl diphenylphosphine oxide, TPO, PEGDA, hydroxiapatite, photoinitiator, extraction.

Introduction. The application of 3D printed orthopedic implants has attracted interest due to their possibilities in personalized medicine. Bioceramics [1], bioglasses [2, 3], metal alloys [4], polymers [5], and their composites [6–8] are used to create implants for bone regeneration. Biocompatibility, hydrophilicity, bioactivity, osteoconductivity, and osteoinductivity are factors that influence the success of the implants [9].

It must also possess mechanical properties that closely align with those of natural bone to ensure the implant can endure the stresses and strains it will withstand [10]. Polyethylene glycol diacrylate (PEGDA) is one such material that has been widely used in the production of 3D-printed orthopedic implants [11]. PEGDA is a biocompatible and hydrophilic polymer that can be readily processed using 3D printing techniques. It possesses a distinctive combination of characteristics that make it an ideal material for orthopedic applications. Firstly, PEGDA is biocompatible, indicating that it is non-toxic and does not trigger any harmful immune

* E-mail: mikayel.torosyan.5@gmail.com

reactions when inserted into the body. Secondly, PEGDA is hydrophilic, allowing the implant to be hydrated, which can improve its mechanical properties and enhance comfort for the patient [12–14]. The mechanical characteristics of PEGDA can be modified by altering the degree of polymerization and crosslinking [15].

Another way to improve the mechanical characteristics and bioactivity of PEDGA is through its combination with hydroxyapatite (HA). HA acts as a reinforcing agent, increasing the compressive modulus, while reducing the swelling degree and degradation rate, thereby enhancing structural stability. Rheologically, HA increases viscosity and shear-thinning behavior. Biologically, HA enhances cell adhesion and osteogenic differentiation by promoting alkaline phosphatase activity and calcium deposition, though excessive HA can slightly reduce cell viability due to ion release. Thus, HA incorporation optimizes PEGDA for bone tissue engineering, balancing mechanical integrity, bioactivity, and printability [16–18].

Nevertheless, the polymerization of PEGDA necessitates a photoinitiator. One of the most frequently utilized photoinitiators is TPO. Despite its effectiveness, TPO is toxic, and any unreacted TPO must be removed from the final product to ensure its safety for use [19].

TPO belongs to a group of compounds called photoinitiators, which are materials that react to light exposure, generating reactive species capable of initiating the polymerization process [20]. Photoinitiators like TPO are crucial in light-induced polymerization processes. They allow for the controlled initiation of the polymerization process, enabling the formation of polymers with desired properties. Although they play an essential role in the polymerization process, photoinitiators such as TPO have their limitations. A primary issue related to the use of TPO is its toxicity, which can result in a variety of adverse effects, ranging from mild irritation to serious health problems [21, 22]. It helps to initiate the polymerization process and allows for the adjustment of the properties of polymers.

The study examined the polymerization dynamics and the efficiency of TPO extraction in PEGDA-based systems using 96% ethanol and saline, with and without the incorporation of HA, through Raman spectroscopy and extraction analysis.

Materials and Methods. PEGDA oligomer (M_n = 575 *g*/*mol*, MDL Number: MFCD00081876, “Sigma Aldrich”, Germany), TPO (97%, MDL Number: MFCD00192110, “Sigma Aldrich”), and HA (≥ 90%, “Sigma Aldrich”) were used as raw materials. The effect of photoinitiator concentration on the polymerization of PEGDA was investigated using five different weight ratios of TPO to PEGDA monomer: 0.05%, 0.1%, 0.2%, 0.3%, and 0.4%. To ensure complete dissolution of the photoinitiator, the PEGDA monomer and TPO were mixed at a controlled temperature of 35℃ using a magnetic stirrer at 700 *rpm* for 30 *min*. Each mixture was then transferred into small cuvettes measuring 15 *mm* × 20 *mm* × 20 *mm*, which essentially acted as molds for shaping the final polymer. Subsequently, the cuvettes were placed inside a UV curing chamber (Form Cure, Formlabs) with a specified emission power of 9 *W*. These chambers utilize light sources emitting a wavelength of 405 *nm*, which efficiently triggers the initiation process (TPO degradation [22]). The curing process was carried out at 35℃ to minimize potential

thermal degradation of the PEGDA monomer [15]. The irradiation time was varied across four durations: 5, 10, 20, and 30 *min*.

The HA composite was synthesized using a procedure very similar to that of the pure polymer, with the addition of an HA incorporation step. HA powder was meticulously introduced into the TPO-PEGDA mixture in portions while stirring with a magnetic stirrer set at 1 000 *rpm* for 30 *min*. The amount of HA constituted 37 wt.% of the entire mixture. This specific weight ratio was chosen based on preliminary studies that balanced the desired mechanical properties [23]. Saline and 96% ethanol were chosen for the extraction of residual unreacted TPO and monomer. Ethanol is a well-established solvent for unreacted PEGDA monomers and residual or potentially unreacted TPO molecules. Saline was included in the extraction solution to mimic physiological conditions. The cuvettes containing the polymer/ composite were submerged in 15 *mL* of the solvent solution within a chamber maintained at 40°C. The extraction process continued for a total of six days with constant stirring at 100 *rpm*. To maximize extraction efficiency and remove the majority of unreacted TPO molecules, the solvent was replaced every 24 *h*.

After the extraction step, the remaining polymer and composite were subjected to various analytical techniques to assess their properties. The extracted solutions were analyzed using a T60UV-Visible spectrophotometer to quantify the amount of TPO removed during the extraction process. Raman spectroscopy was performed using a HORIBA XploRA^{TM} PLUS Raman spectrometer to characterize the polymerization degree of the polymer. This non-destructive technique provides valuable information about the presence of specific functional groups within the material [24].

Results and Discussion. Following the photopolymerization process, a thin layer of viscous liquid was observed on the polymer surface. Raman spectroscopy analysis (Fig. 1) revealed that this was a layer of partially polymerized PEGDA monomer. Characteristic peaks in the spectrum confirmed this, with the peaks at 1634 cm^{-1} and 1729 cm^{-1} corresponding to the carbon-carbon double bond (C=C) and the carbon-oxygen double bond (C=O) of the acrylate group within the PEGDA monomer, respectively.

These observations suggest incomplete polymerization at the material's surface, a phenomenon known as surface termination in radical chain reactions [25]. During radical photopolymerization, a series of reactions leads to polymer chain propagation. However, when the reaction occurs at the surface, the photoinitiator can react not only with the desired PEGDA monomers but also with surrounding materials like the cuvette mold or oxygen from the air. These unintended reactions can quench the propagating radicals, effectively halting polymerization at the very surface.

The presence of strong peaks corresponding to the C=C double bond in the Raman spectrum of the unreacted monomer layer supports this conclusion. As the sampling spot was moved deeper into the polymerized material, the peak intensity gradually decreased, eventually disappearing around 100–200 μm depth.

The peak height of the C=C bond serves as an indicator of the degree of polymerization. A lower peak intensity signifies a higher degree of polymerization (Fig. 1). It was observed that the peak height of the C=C bond is inversely proportional to the TPO concentration. The literature describes the relationship

between the conversion of the monomer and the concentration of the photoinitiator. This suggests that a higher TPO concentration, which leads to a faster initial reaction rate, may not necessarily result in a more extensively polymerized product at the surface due to the potential dominance of unintended termination reactions [23].

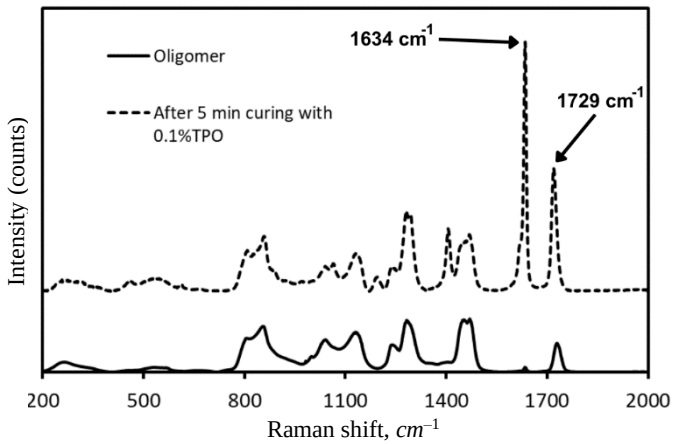

Fig. 1. The Raman spectra of PEGDA 575 oligomer and polymer cured for 5 *min* using 0.1% TPO.

The band corresponding to the C=O stretching vibration experiences a shift of 10 cm^{-1} in the polymer compared to the monomer. This can be attributed to the loss of conjugation. In the monomer, the C=C bond is conjugated with C=O, spreading two π electron clouds across four carbon atoms. This increases the stability of the molecule but weakens the C=O and C=C bonds. During polymerization, the C=C bond enters the reaction, leading to a loss of conjugation. As a result, the C=O bond strengthens, which is why a shift of the C=O band to the higher wavenumber (energy) region by 10 cm^{-1} can be observed. The C=C band does not shift as we only observe peaks from the monomer. Additionally, the C=O band broadens in the polymer spectrum, indicating the presence of the C=O peak originating from the monomer.

Effect of TPO Concentration and Curing Time. The curing time appears to have a more significant impact on the volume of polymerized material rather than the overall degree of polymerization within the reacted regions. As shown in Fig. 2 for the HA composite, after only 5 *min* of curing, the polymerization process appeared to be stopped at a certain depth. Conversely, with a 30-minute curing time, the entire volume of the mixture had reacted.

As can be seen from Fig. 2, the propagation and termination reactions rates differ for various photoinitiator concentrations. At lower concentrations the polymerized mass wall thickness is thicker (Fig. 2, a and b), which indicates that the propagation reaction is more dominant compared to higher concentrations. At higher concentrations the walls are thinner (Fig. 2, c and d). This phenomenon can be observed also at the molecular level which was investigated with Raman spectrometer [24].

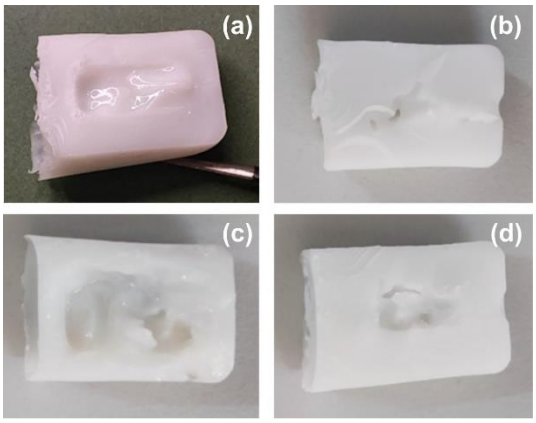

Fig. 2. The images of polymerized samples using various curing time and concentration of TPO in PEGDA/HA composite:

a) 0.1% – 5 *min*; b) 0.1% – 30 *min*;
c) 0.4% – 5 *min*; d) 0.4% – 30 *min*.

The degree of conversion (DOC) can be assessed by analyzing the peak intensities of the C=C and C=O bonds in the Raman spectra. Equation illustrates the relationship between DOC and peak intensities [23, 26]. Future studies could explore this approach to determine the optimal curing time and TPO concentration for achieving a well-defined and controlled polymerization profile across the material. Calculation of degree of conversion:

$$\mathrm{DOC} = 1 - \frac{I_{(\mathrm{C=C})}/I_{(\mathrm{C=O})}}{I_{L(\mathrm{C=C})}/I_{L(\mathrm{C=O})}}.$$

Here, $I_{(\mathrm{C=C})}$ and $I_{(\mathrm{C=O})}$ are intensities of the polymer; $I_{L(\mathrm{C=C})}$ and $I_{L(\mathrm{C=O})}$ are intensities of monomer. Using this equation has been plotted the dependency of curing time and DOC (Fig. 3).

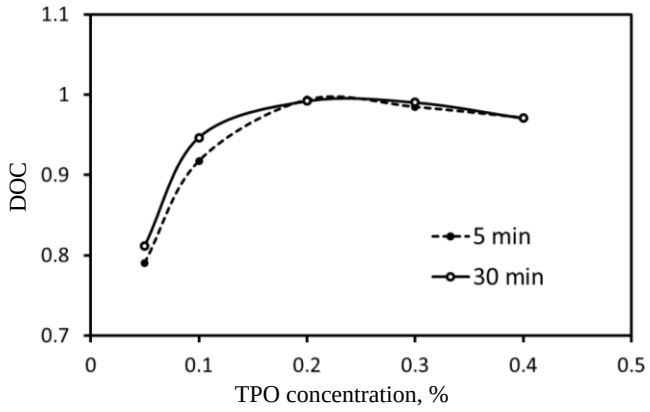

Fig. 3. The degree of conversion dependency on concentration and curing time.

The DOC values differ depending on the curing time when TPO concentration is 0.05% and 0.1% (Fig. 3). At a TPO concentration of 0.2%, the DOC reaches its highest value for both 5- and 30-minutes curing. With increasing TPO concentration (over 0.2%), the DOC does not change significantly with the curing duration. The decrease in DOC at higher TPO concentrations is caused by kinetics of different steps of the polymerization reaction: particularly the propagation and termination reactions steps. Increasing the concentration of TPO leads to the formation of higher number of growing chains, which results in an elevated rate of termination reactions.

Consequently, the forming chains are shorter and the concentration of C=C is higher. The curing time also influences the DOC at low TPO concentration. This can be explained by change in the diffusion rate. As the polymerization reaction leads to an increase in viscosity, the monomer molecules need more time to reach the growing chain. After a certain concentration, the probability to meet growing chain is much more difficult, so additional curing time will not lead to an increase in DOC, as can be observed on the graph.

Extraction of TPO. The efficiency of TPO extraction from the final polymer was investigated using two solvents: saline and 96% ethanol solution. A series of experiments were conducted to evaluate the extraction efficiency from the PEGDA matrix. Firstly, the changes in UV spectra were investigated for TPO (Fig. 4). As it can be seen from the Fig. 4, the peaks at 266 *nm* and 275 *nm* are not changed after curing and are selected as TPO specific peaks for further analysis.

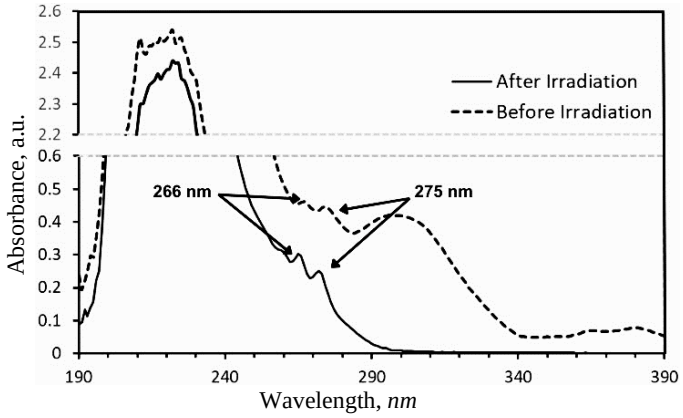

Fig. 4. The UV spectra of TPO before and after curing.

The samples obtained using different quantities of TPO (0.05%, 0.1%, 0.2%, 0.3%, 0.4%) and cured for 5 *min* and 30 *min* were immersed in ethanol and saline. Both solvents containing extracted TPO were eliminated from the vessels, and new solutions were added. The concentration of extracted TPO in the solutions was studied for 6 days. Fig. 5 illustrates the intensity of the specific peak of extracted TPO of samples cured for 5 *min* and 30 *min* using 0.1 % TPO. Samples containing 0.2%, 0.3% and 0.4% TPO have the same behavior in the solvents.

As illustrated in Fig. 5, the concentration of TPO in the solvents declines according to a logarithmic function. On the sixth day, the concentration approaches minimal levels. The R^2 is around 0.97 and 0.98 for both samples extracted in ethanol, which verifies the validity of the method. The R^2 for saline is lower because of the low concentration of TPO extracted. Hence the signal-to-noise ratio in this case is not big. This proves that the extraction efficiency for the saline and 96% ethanol solution is drastically different from each other, as the solubility of TPO and its by-products is much higher in ethanol than in saline. It should be noted that the samples cured for 5 *min*.

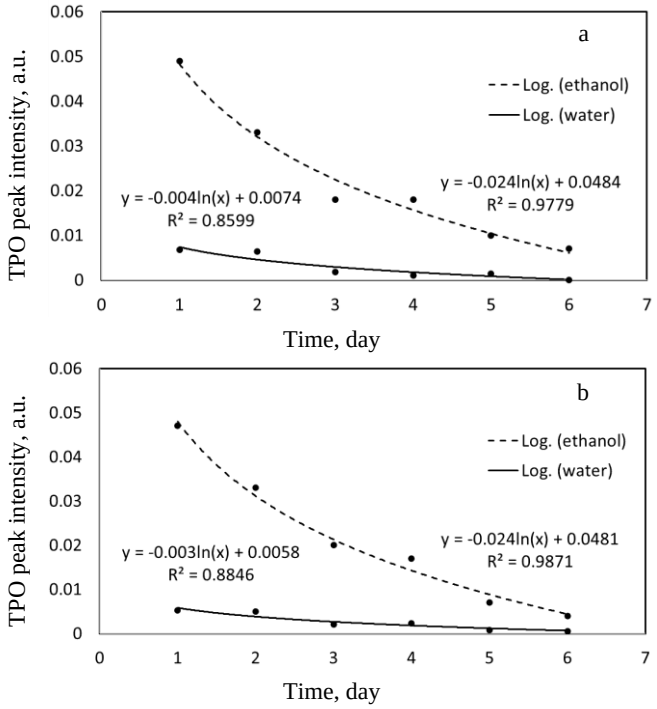

Fig. 5. The intensity of extracted TPO peaks in ethanol and saline for the samples cured: a) 5 *min*, b) 30 *min*.

The intensity of TPO extracted in ethanol is somewhat elevated for samples cured for 5 *min*. This is due to the impact of curing time, which was previously mentioned: the duration of curing has a minimal effect on the polymerization degree.

Conclusion. Raman analysis revealed that the DOC was predominantly influenced by TPO concentration rather than curing time. On the other hand, high concentrations of TPO led to a higher number of growing chains, which elevated the rate of termination reactions. Consequently, the forming chains were shorter. On the surface, incomplete polymerization was observed due to environmental factors, including oxygen interference, which caused radical chain termination.

The incorporation of HA significantly affected the polymerization behavior. In these systems, irradiation time became more critical than TPO concentration. HA restricted the diffusion of radicals, leading to localized termination reactions at higher TPO concentrations. Conversely, lower concentrations of TPO allowed radicals sufficient time to diffuse and propagate, resulting in improved polymerization.

The study of TPO extraction efficiency highlighted superior performance of ethanol solutions compared to saline. The higher solubility of TPO and its by-products in ethanol ensured more efficient extraction. Additionally, polymers subjected to 5 *min* of UV irradiation exhibited a slightly higher TPO concentrations in the extracted solution than those irradiated for 30 *min*. This minor difference was attributed to the marginally higher number of reactions occurring with prolonged irradiation, although the effect was minimal. In future work, the integration of antibiotics into the system will be explored. Since these antibiotics will likely be in the form of HCl salts, they will be soluble in water but not in ethanol.

This means that after printing, implants can first be cleaned with ethanol to effectively remove TPO.

This work was supported by the Science Committee of the MESCS RA, in the frames of the research project No. 23AA-2F039 and 22IRF-05.

Received 07.10.2025
Reviewed 19.11.2025
Accepted 25.11.2025

REFERENCES

1. Rodriguez C.A., Lara-Padilla H., Dean D. Bioceramics for Musculoskeletal Regenerative Medicine: Materials and Manufacturing Process Compatibility for Synthetic Bone Grafts and Medical Devices. *3D Printing and Biofabrication* (2018), 161–183. https://doi.org/10.1007/978-3-319-45444-3_22
2. Sultan S., Thomas N., et al. The Design of 3D-Printed Polylactic Acid–Bioglass Composite Scaffold: A Potential Implant Material for Bone Tissue Engineering. *Molecules* **27** (2022), 7214. https://doi.org/10.3390/molecules27217214
3. Rajzer I., Kurowska A., et al. 3D-Printed Polycaprolactone Implants Modified with Bioglass and Zn-Doped Bioglass. *Materials* **16** (2023), 1061. https://doi.org/10.3390/ma16031061
4. Wua Yu., Liua J., et al. An Overview of 3D Printed Metal Implants in Orthopedic Applications: Present and Future Perspectives. *Heliyon* **9** (2023), e17718.
5. https://doi.org/10.1016/j.heliyon.2023.e17718
6. Picco C.J., Utomo E., Development of 3D-Printed Subcutaneous Implants Using Concentrated Polymer/drug Solutions. *Intern. J. of Pharm.* **631** (2023), 122477. https://doi.org/10.1016/j.ijpharm.2022.122477
7. Montazerian M., Hosseinzadeh F., et al. Bioceramic Coatings on Metallic Implants: An Overview. *Ceramics International* **48** (2022), 8987–9005. https://doi.org/10.1016/j.ceramint.2022.02.055
8. Li X., Heidari A., et al. Design and Fabrication of Elastic Two-Component Polymer-Metal Disks Using a 3D Printer under Different Loads for the Lumbar Spine. *Polymer Testing* **112** (2022), 107633. https://doi.org/10.1016/j.polymertesting.2022.107633
9. Ma H., Feng C., et al. 3D-printed Bioceramic Scaffolds: From Bone Tissue Engineering to Tumor Therapy. *Acta Biomaterialia* **79** (2018), 37–59. https://doi.org/10.1016/j.actbio.2018.08.026
10. Huang H., Xiang C., et al. Patient-Specific Geometrical Modeling of Orthopedic Structures with High Efficiency and Accuracy for Finite Element Modeling and 3D Printing. *Australasian Physical & Engineering Sciences in Medicine* **38** (2015), 743–753. https://doi.org/10.1007/s13246-015-0402-1
11. Rekowska N., Huling J., et al. Mechanical and Biocompatibility Analyses of Photochemically Polymerized PEGDA250 for Photopolymerization-Based Manufacturing Processes. *Pharmaceutics* **14** (2022), 628. https://doi.org/10.3390/pharmaceutics14030628
12. Khalili M.H., Zhang R., et al. Additive Manufacturing and Physicomechanical Characteristics of PEGDA Hydrogels: Recent Advances and Perspective for Tissue Engineering. *Polymers* **15** (2023), 2341. https://doi.org/10.3390/polym15102341
13. Chapla R., Abed M.A., West J.L. Modulating Functionalized Poly(ethylene glycol) Diacrylate Hydrogel Mechanical Properties Through Competitive Crosslinking Mechanics for Soft Tissue Applications. *Polymers* **12** (2020), 3000. https://doi.org/10.3390/polym12123000

14. Nemir S., Hayenga H.N., West J.L. PEGDA Hydrogels with Patterned Elasticity: Novel Tools for the Study of Cell Response to Substrate Rigidity. *Biotechnology and Bioengineering* **105** (2009), 636–644. https://doi.org/10.1002/bit.22574
15. Priola A., Gozzelino G., et al. Properties of Polymeric Films Obtained From u.v. Cured Poly(ethylene glycol) Diacrylates. *Polymer* **34** (1993), 3653–3657. https://doi.org/10.1016/0032-3861(93)90050-K
16. Paxton J.Z., Donnelly K., et al. Engineering the Bone-ligament Interface Using Polyethylene Glycol Diacrylate Incorporated with Hydroxyapatite. *Tissue Engineering, Part A* **15** (2008). https://doi.org/10.1089/ten.tea.2008.0105
17. Deng X., Huang B., et al. 3D Printing of Robust and Biocompatible Poly(ethylene glycol)diacrylate/nano-hydroxyapatite Composites via Continuous Liquid Interface Production. *Journal of Materials Chemistry B* **5** (2021). https://doi.org/10.1039/D0TB02182B
18. Rajabi M., Cabral J.D., et al. Development and Optimization of Hydroxyapatite-polyethylene Glycol Diacrylate Hydrogel inks for 3D Printing of Bone Tissue Engineered Scaffolds (2023). *Biomedical Materials* **18** (2023), 065009. https://doi.org/10.1088/1748-605X/acf90a
19. de Melo Soares V., dos Reis A.C., da Costa Valente M.L. The Influence of 2,4,6-Trimethyl-benzoyldiphenylphosphine Oxide on the Toxicity of Dental Resins: A Systematic Review of *in vitro* Studies. *International Journal of Adhesion and Adhesive*s **138** (2025), 103922. https://doi.org/10.1016/j.ijadhadh.2024.103922
20. Sluggett G.W., Turro C., et al. (2,4,6-Trimethylbenzoyl)diphenylphosphine Oxide Photochemistry. A Direct Time-Resolved Spectroscopic Study of Both Radical Fragments. *Journal of the American Chemical Society* **117** (1995), 5148–5143. https://doi.org/10.1021/ja00123a018
21. Leprince J.G., Hadis M., et al. Photoinitiator Type and Applicability of Exposure Reciprocity Law in Filled and Unfilled Photoactive Resins. *Dental Materials* **27** (2011), 157–164. https://doi.org/10.1016/j.dental.2010.09.011
22. Popal M., Volk J., et al. Cytotoxic and Genotoxic Potential of the Type I Photoinitiators BAPO and TPO on Human Oral Keratinocytes and V79 Fibroblasts. *Dental Materials* **34** (2018),1783–1796. https://doi.org/10.1016/j.dental.2018.09.015
23. Zhang Zh.F., Ma Xi., et al. Influence of Polymerization Conditions on the Refractive Index of Poly (ethylene glycol) Diacrylate (PEGDA) Hydrogels. *Appl. Phys. A* **124** (2018), 283. https://doi.org/10.1007/s00339-018-1713-3
24. Kudelski A. Analytical Applications of Raman Spectroscopy. *Talanta* **76** (2008), 1–8. https://doi.org/10.1016/j.talanta.2008.02.042
25. Andrzejewska E. Free Radical Photopolymerization of Multifunctional Monomers *Micro and Nano Technologies* (2016), 62–81. https://doi.org/10.1016/B978-0-323-35321-2.00004-2
26. Alketbi A.S., Shi Yu., et al. Impact of PEGDA Photopolymerization in Micro-Stereolithography on 3D Printed Hydrogel Structure and Swelling. *Soft Matter* **30** (2021). https://doi.org/10.1039/D1SM00483B
27. Jessop J.L.P. A Practical Primer: Raman Spectroscopy for Monitoring of Photopolymerization. *Polymers* **15** (2023), 3835. https://doi.org/10.3390/polym15183835

Մ. Ս. ԹՈՐՈՍՅԱՆ

ՏՐԻՄԵԹԻԼԲԵՆԶՈՒԼ ԴԻՖԵՆԻԼՖՈՍՖԻՆՕՔՍԻԴԻ ԼՈՒԾԱՀԱՆՈՒՄԸ ԹՐԾՎԱԾ PEGDA-ՀԻԴՐՕՔՍԻԱՊԱՏԻՏ ՈՍԿՐԱՅԻՆ ԻՄՊԼԱՆՏԻՑ

Անհատականացված իմպլանտները գնալով ավելի տարածված են դառնում, և ադդիտիվ արտադրությունը ամենաարդյունավետ լուծումներից

մեկն է: Բազմաթիվ հետազոտություններ են նվիրված մեխանիկական հատկությունների բարելավմանը՝ միաժամանակ պահպանելով կենսահամատեղելիությունը: Իմպլանտների տպագրության համար հաճախ օգտագործվող պոլիմեր է պոլիէթիլենգլիկոլ դիակրիլատը (PEGDA), որը նաև օգտագործվում է որպես հակաբիոտիկների հիմք՝ կանխելով դրանց օրալ ընդունումը և նվազեցնելով դրանց բացասական ազդեցությունը մարդու մարմնի վրա: PEGDA-ի պոլիմերացման համար օգտագործվող ամենատարածված ֆոտոհարուցիչներից մեկը տրիմեթիլբենզոիլ դիֆենիլֆոսֆինօքսիդն է (TPO), որը վտանգավոր է: Այս ուսումնասիրության նպատակն էր մշակել TPO-ն իմպլանտից ընտրողաբար հեռացնելու մեթոդ՝ հակաբիոտիկը պահպանելու և հնարավոր վտանգները նվազեցնելու համար: Օգտագործվել են երկու լուծիչ՝ ֆիզիոլոգիական լուծույթ և 96% էթանոլ: Էթանոլը ցույց է տվել ավելի բարձր արդյունավետություն TPO-ն պոլիմերային մատրիցից լուծահանելուց՝ միաժամանակ պահպանելով հակաբիոտիկի պարունակությունը: Սա ցույց է տալիս, որ հնարավոր է TPO-ն հեռացնելու իմպլանտից ընտրողաբար, նվազագույնի հասցնելով հնարավոր ռիսկերը:

М. С. ТОРОСЯН

ИЗВЛЕЧЕНИЕ ТРИМЕТИЛБЕНЗОИЛДИФЕНИЛФОСФИНОКСИДА ИЗ ОТВЕРЖДЕННОГО КОСТНОГО ТРАНСПЛАНТАТА PEGDA-ГИДРОКСИАПАТИТА

В настоящее время персонализированные имплантаты становятся все более интересной темой, а аддитивное производство является одним из наиболее эффективных решений. Многочисленные исследовательские работы посвящены улучшению механических свойств при сохранении биосовместимости. Часто используемым полимером для печати имплантатов является полиэтиленгликольдиакрилат (PEGDA), который также используется в качестве основы для антибиотиков, предотвращая их пероральный прием и снижая их негативное воздействие на организм человека. Одним из наиболее распространенных фотоинициаторов, используемых для полимеризации PEGDA, является триметилбензоилдифенилфосфиноксид (TPO), который является опасным. Целью данного исследования является изучение метода селективного удаления TPO из имплантата для снижения потенциальной опасности и сохранения содержания антибиотика. Были использованы два растворителя: физиологический раствор и 96% раствор этанола. В результате этанол демонстрировал более высокую эффективность экстракции TPO из полимерной матрицы при сохранении содержания антибиотика. Это свидетельствует о возможности селективной экстракции TPO из имплантата, что минимизирует потенциальные риски.